

## Research Article

# Synthesis and Luminescence Properties of $\text{SrGd}_2\text{O}_4:\text{Eu}^{3+}$ Red Phosphors

Jun-Feng Wang <sup>1</sup>, Hao Zu <sup>1</sup>, Chuan-Wen Lin <sup>2</sup>, Shou-Jun Ding <sup>3</sup>, Peng-Yu Shao,<sup>3</sup>  
and Ye Xia<sup>3</sup>

<sup>1</sup>School of Advanced Manufacturing Engineering, Hefei University, Hefei 230601, China

<sup>2</sup>School of Artificial Intelligence and Big Data, Hefei University, Hefei 230601, China

<sup>3</sup>School of Mathematics and Physics, Anhui University of Technology, Maanshan 243032, China

Correspondence should be addressed to Hao Zu; haozu@hust.edu.cn, Chuan-Wen Lin; lincw@hfu.edu.cn, and Shou-Jun Ding; sjding@ahut.edu.cn

Received 22 November 2019; Accepted 10 February 2020; Published 14 April 2020

Academic Editor: Sulaiman W. Harun

Copyright © 2020 Jun-Feng Wang et al. This is an open access article distributed under the Creative Commons Attribution License, which permits unrestricted use, distribution, and reproduction in any medium, provided the original work is properly cited.

As one of the important raw materials for LED products, phosphors play an important role. At present, the spectrum of LED phosphors lacks red light, resulting in poor quality of white LED products and a low color rendering index ( $R_a < 80$ ), which affects lighting effects. To solve this problem, we synthesized the  $\text{SrGd}_2\text{O}_4:\text{Eu}^{3+}$  red phosphor by a high-temperature solid-phase method. The structure and luminescence properties of  $\text{SrGd}_2\text{O}_4:\text{Eu}^{3+}$  red phosphors were studied by means of X-ray diffraction (XRD) measurements of their emission and excitation spectra, and their spectra were analyzed. We also studied the  $\text{Eu}^{3+}$  doping concentration with the best luminous efficiency and the color coordinate of the  $\text{SrGd}_2\text{O}_4:\text{Eu}^{3+}$  phosphor. The experimental results show that  $\text{SrGd}_2\text{O}_4:\text{Eu}^{3+}$  is a new red phosphor material that can be used for near-ultraviolet or blue-light excitation and has good practicability.

## 1. Introduction

With the global climate change and the background of energy crisis, the awareness of environmental protection and energy conservation is becoming more and more important. Because LED (light-emitting diode) has the advantages of durability, energy conservation, fast response, compactness, strong anti-interference ability, high brightness, no mercury pollution, and environmental protection, it is becoming a trend in lighting [1, 2].

The way in which the LED realizes white light is mainly by mixing a light-emitting chip and phosphors that can be activated by the light-emitting chip. Since the phosphor degrades during use and affects the quality of light, the phosphor material is the key to ensuring the quality of LED products [3]. Commercially produced white LEDs require red phosphors to be added to compensate for the lacking of red light components [4, 5].

The currently used red phosphors remain at the traditional level of rare earth ion-activated sulfide substrates, and

their synthesis and application generally have the following problems: (1) The optimal excitation wavelength of the red phosphor cannot closely match with the emission wavelength of the blue chip, resulting in a low red light excitation rate [5, 6]. (2) The red phosphor itself has low luminous efficiency and poor application effect [7]. (3) When the red phosphor is effectively excited, its emission spectrum range is narrow, and the compensation effect on light is poor [8, 9]. (4) Whether the matching of the red phosphor matrix with the widely used yellow phosphor matrix affects the respective luminescence interaction remains to be studied. In addition, conventional red fluorescence based on sulfide substrates may produce toxic substances during the synthesis process [10–12].

Recently, the investigation of red phosphor matrix is mainly divided into the following types: (1) nitride or nitrogen oxide matrix, which has excellent thermal stability, chemical stability, and good controllability; it has been widely studied, and  $\text{Eu}^{2+}$  is usually used as an activating ion. However, the requirements for the preparation conditions of

the nitride red phosphor are very strict, generally high temperature up to  $1400^{\circ}\text{C}\sim 2000^{\circ}\text{C}$ , long-term insulation, and need to be protected under nitrogen. This will inevitably increase the cost of the phosphor and consume a lot of resources, which is a disadvantage for commercial production [13, 14]. (2) Borate matrix, which is easy to synthesize and stable in physical and chemical properties. However, it has shortcomings such as short emission wavelength and serious aging phenomenon [15]. (3) Silicate matrix, which has good light permeability, high luminous efficiency, and low production cost, but the silicate itself has poor chemical stability, and it is necessary to study whether it can widely use white LED [16]. (4) Aluminate matrix, which has a high quantum conversion rate and the color of the light is stable [17]. However, there are few research reports on the red phosphor of the matrix.

In summary, the traditional commercial phosphors  $\text{CaS:Eu}^{3+}$ ,  $\text{Y}_2\text{O}_2\text{S:Eu}^{3+}$  et al have shortcomings such as low luminous efficiency, poor stability and short life [18, 19]. Recently, researchers are exploring new red phosphor materials to study the effects of different matrices and different doping ions on the luminescence properties of fluorescent materials [20–22]. It can be foreseen that the luminescent properties of red phosphors will be making big progress. In this study,  $\text{SrGd}_2\text{O}_4$  was chosen as the new luminescent matrix material. The  $\text{SrGd}_2\text{O}_4:\text{Eu}^{3+}$  phosphor was synthesized by a high-temperature solid-phase method, and the relationship between luminescence properties and concentration was explored.

## 2. Principle and Experiment

Fluorescence is a process that produces light with little heat compared to thermal radiation. A suitable material absorbs high-energy radiation, which in turn emits light, the energy of which is lower than the energy of the excitation radiation. When the luminescent material is a solid, the material is commonly referred to as a phosphor. The high-energy radiation that excites the phosphor may be electrons or ions with high velocity, or photons ranging from gamma rays to visible light.

Figure 1 shows the unit cell structure of  $\text{SrGd}_2\text{O}_4$ . It can be seen from the figure that strontium is equipped with six oxygen atoms in a unit cell to form a triangular prism, which is in the center of inversion symmetry. The gadolinium is equipped with six oxygens in one unit cell to form an octahedron in the center of noninversion symmetry.

In this work,  $\text{SrGd}_2\text{O}_4:\text{Eu}^{3+}$  phosphors were synthesized by the high-temperature solid-phase method. The raw materials  $\text{Eu}_2\text{O}_3$ ,  $\text{Gd}_2\text{O}_3$ , and  $\text{SrCO}_3$  were weighed accurately according to stoichiometric ratios. The doping concentrations of  $\text{Eu}^{3+}$  are 1%, 2%, 5%, 10%, and 15%, respectively. The agate mortar was wiped with alcohol cotton, and the raw materials were separately mixed in a mortar, and each group was thoroughly ground for 30 minutes. Then, the ground mixtures were loaded in a clean crucible and placed in a furnace. The reaction temperature and time were set as  $1400^{\circ}\text{C}$  and 48 hours, respectively. Lastly, the samples were cooled down to room temperature naturally and thoroughly ground.

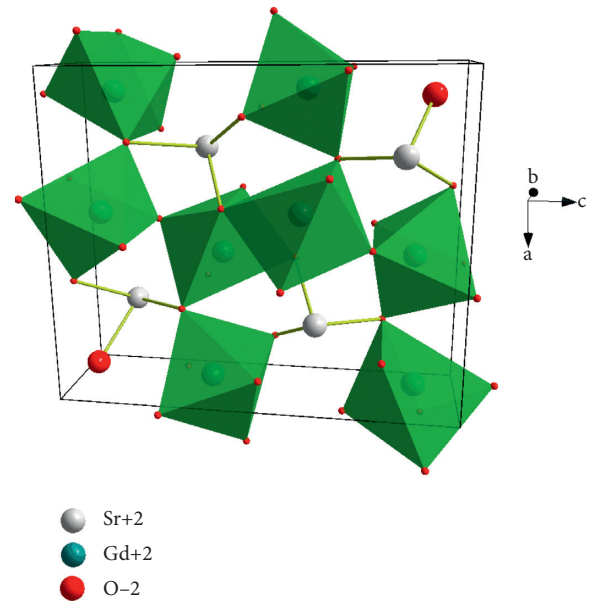


FIGURE 1: The cell structure of  $\text{SrGd}_2\text{O}_4$ .

A Philips X' pert Pro X-ray powder diffractometer equipped with  $\text{Cu K}\alpha$  radiation was employed to determine the crystal structure. In the measured  $2\theta$  range ( $10^{\circ}$  to  $90^{\circ}$ ), the scan step was set as  $0.033^{\circ}$ . An Edinburgh FLSP-920 spectrometer was used to measure the excitation and emission spectra of the samples. The international CIE 1931 standard chromaticity system was used to draw the chromaticity coordinate diagram of the phosphor.

## 3. Results and Discussion

Figure 2 shows the XRD pattern of the as-synthesized  $\text{SrGd}_2\text{O}_4:\text{Eu}^{3+}$  phosphors with different  $\text{Eu}^{3+}$  doping concentrations (1%–15%). Compared with the data from the standard card of  $\text{SrGd}_2\text{O}_4$  (card number: ICSD#150876), the as-synthesized samples are coincident well with them, indicating that the structure of  $\text{SrGd}_2\text{O}_4$  is unaffected by the doping of  $\text{Eu}^{3+}$ . In addition, the diffraction peaks of the synthesized samples with different concentrations are symmetrical and sharp, indicating that the as-synthesized samples are well crystalline.

Figure 3 shows the excitation spectrum of the 2 at%  $\text{Eu}^{3+}$ -doped  $\text{SrGd}_2\text{O}_4$  phosphor at room temperature. The excitation spectrum of the sample consists of a series of peaks. In the wavelength range of 240 nm to 330 nm, charge transfer of  $\text{O}^{2-}\rightarrow\text{Eu}^{3+}$  is generated, and the charge migrates from the 2p orbital of  $\text{O}^{2-}$  to the 4f orbital of the central metal ion  $\text{Eu}^{3+}$ . The  $\text{Eu}^{3+}$  samples also have strong excitation peaks at 370 nm, 380 nm, and 400 nm, respectively.  ${}^7\text{D}_0\rightarrow{}^5\text{D}_4$  transitions occur around 370 nm,  ${}^7\text{D}_0\rightarrow{}^5\text{G}_2$  transitions occur around 380 nm, and  ${}^7\text{D}_0\rightarrow{}^5\text{L}_6$  transitions occur around 400 nm. It shows that the phosphor can be effectively excited by near-ultraviolet light and blue light, so it can be used as a red phosphor component excited by the near-ultraviolet LED chip and blue LED chip.

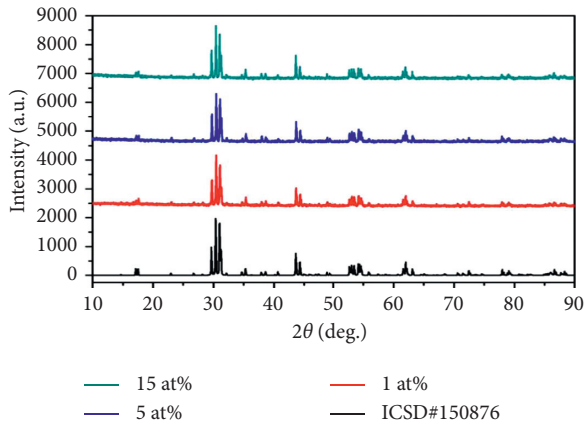


FIGURE 2: The XRD patterns of (1 at%, 5 at%, and 15 at%) SrLa<sub>2</sub>O<sub>4</sub>:Eu<sup>3+</sup>.

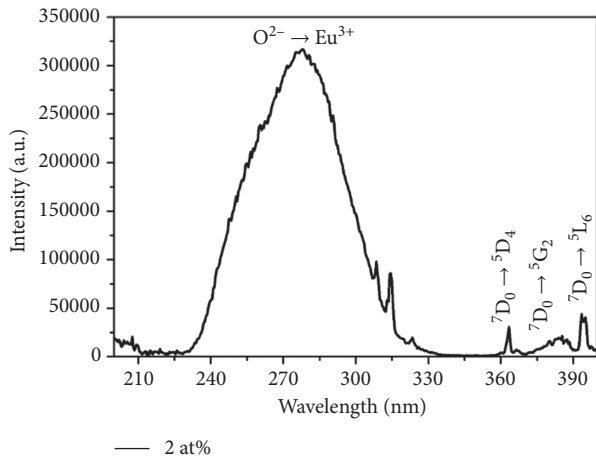


FIGURE 3: The excitation spectra of (1 at%) SrGd<sub>2</sub>O<sub>4</sub>:Eu<sup>3+</sup> phosphor.

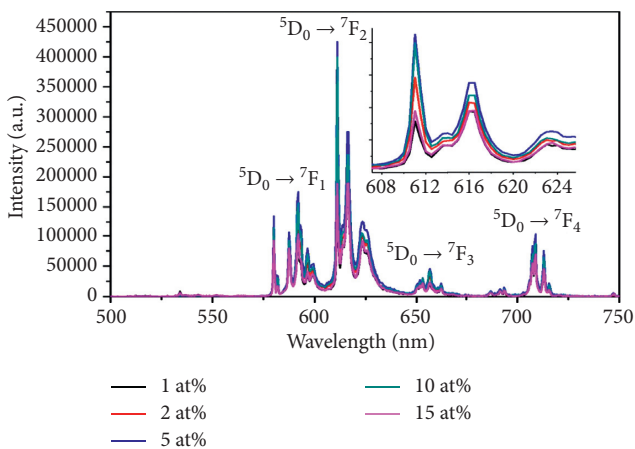


FIGURE 4: The emission spectra of SrGd<sub>2</sub>O<sub>4</sub>:Eu<sup>3+</sup> phosphors with different doping concentrations.

Figure 4 shows the emission spectra of SrGd<sub>2</sub>O<sub>4</sub>:Eu<sup>3+</sup> phosphors with different doping concentrations at room temperature. A series of emission peaks are observed in the

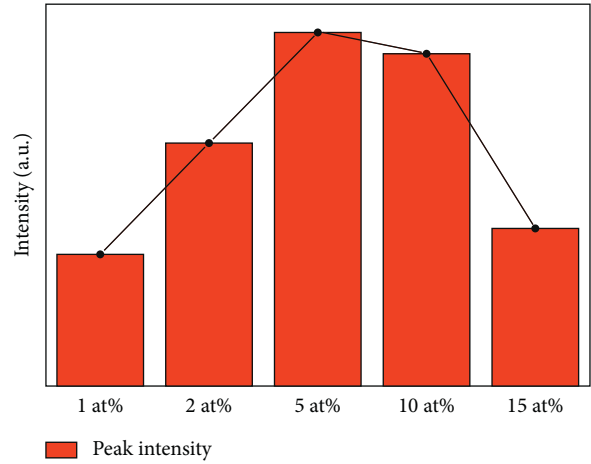


FIGURE 5: The emission peak intensity value of the SrGd<sub>2</sub>O<sub>4</sub>:Eu<sup>3+</sup> phosphor with different doping concentrations.

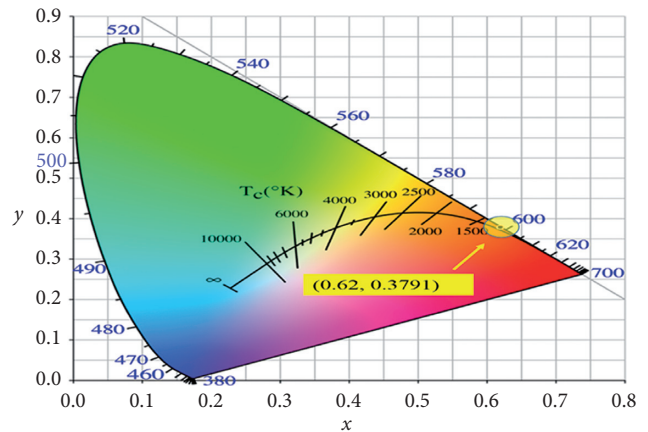


FIGURE 6: The CIE coordinate diagram of the SrGd<sub>2</sub>O<sub>4</sub>:Eu<sup>3+</sup> phosphor.

wavelength range of 580 nm to 720 nm, which are corresponding to the transitions of <sup>5</sup>D<sub>0</sub>→<sup>7</sup>F<sub>1</sub> (orange emission), <sup>7</sup>F<sub>2</sub> (orange emission), <sup>7</sup>F<sub>3</sub> (red emission), and <sup>7</sup>F<sub>4</sub> (red emission), respectively, as denoted in the figure. According to the unit cell structure SrGd<sub>2</sub>O<sub>4</sub> (Figure 2), the gadolinium is in the noninversion symmetry center plus considering the charge balance and radius similarity. It can be concluded that Eu<sup>3+</sup> is most likely to replace Gd<sup>3+</sup>, which coincides with the XRD characterization structure.

Figure 5 shows the emission peak intensity at different doping concentrations of the SrGd<sub>2</sub>O<sub>4</sub>:Eu<sup>3+</sup> phosphor at room temperature. It can be seen that with the increase of Eu<sup>3+</sup> doping concentration, the luminescence intensity of the samples firstly increases and then weakens. When the doping concentration is between 1% and 5%, the luminescence effect of the phosphor can be greatly improved by incorporating Eu<sup>3+</sup>. This is because when the concentration of Eu<sup>3+</sup> is low, it is not possible to form a sufficient luminescent center and the luminescence intensity is not high. When the doping concentration is 5%, the luminescence intensity reaches a peak, and then as the doping concentration increases (5% to 15%), the luminescence intensity

decreases and concentration quenching occurs. This is because when the  $\text{Eu}^{3+}$  concentration exceeds a certain range, the interaction force between  $\text{Eu}^{3+}$  and  $\text{Eu}^{3+}$  is enhanced, which leads to energy transfer efficiency exceeding the energy emission probability, and energy loss is caused by lattice migration.

The international CIE 1931 standard chromaticity system is a two-dimensional planar CIE chromaticity diagram represented by a nominal value ( $X$ ,  $Y$ ), where  $X$  represents the red component and  $Y$  represents the green component. Figure 6 represents a color coordinate diagram of the  $\text{SrGd}_2\text{O}_4:\text{Eu}^{3+}$  phosphor. It can be seen from the figure that a strong red light is emitted at 611 nm under the excitation of 396 nm excitation light, and the color coordinates at this time are (0.62 and 0.3791).

#### 4. Conclusion

In this work,  $\text{SrGd}_2\text{O}_4:\text{Eu}^{3+}$  phosphors were successfully prepared by the high-temperature solid-phase method. By studying its spectral analysis and luminescence properties, the following conclusions can be drawn: (1) the XRD pattern analysis showed that the  $\text{SrGd}_2\text{O}_4:\text{Eu}^{3+}$  crystal synthesized in the laboratory has good structure, and the  $\text{Eu}^{3+}$  doping has little effect on the lattice parameter of  $\text{SrGd}_2\text{O}_4$ . (2) When the  $\text{Eu}^{3+}$  doping concentration is 5%, the  $\text{SrGd}_2\text{O}_4:\text{Eu}^{3+}$  phosphor has the highest luminescence intensity. (3) The  $\text{SrGd}_2\text{O}_4:\text{Eu}^{3+}$  phosphor emits intense red light at 611 nm under the excitation of 267 nm excitation light, and the color coordinates are (0.62 and 0.3791). (4) By analyzing the excitation and emission spectroscopy of the  $\text{SrGd}_2\text{O}_4:\text{Eu}^{3+}$  phosphor, the phosphor can be used together with near-ultraviolet LED chip and blue LED chip to realize white light illumination. In summary, it can be determined that  $\text{SrGd}_2\text{O}_4:\text{Eu}^{3+}$  is a new red phosphor material that can be used for near-ultraviolet or blue-light excitation and has a good effect.

#### Data Availability

The raw material composition and ratio data used to support the findings of this study are currently under embargo while the research findings are commercialized. Requests for data, 12 months after the publication of this article, will be considered by the corresponding author.

#### Conflicts of Interest

The authors declare that they have no conflicts of interest.

#### Acknowledgments

The authors express that they are grateful to Dr. CHEN Zhen-Ting for providing the equipment for the measurements and wish to thank Prof. Feng Chang-Qin for the valuable discussion and recommendation. This study was funded by (1) the Fund of The Key Laboratory of Polarizing Imaging Detection Technology in Anhui Province (2018-KFJJ-04); (2) the Talent Research Fund of Hefei University (18-19RC30, 18-19RC36, and 18-19RC39); (3) the Key

Natural Science Research Projects of Anhui Universities (KJ2019A0839 and KJ2019A0840); and (4) Scientific Research Development Fund of Hefei University (19ZR03ZDA).

#### References

- [1] Y. Feng, J. Huang, L. Liu, J. Liu, and X. Yu, "Enhancement of white-light-emission from single-phase  $\text{Sr}_5(\text{PO}_4)_3\text{F}:\text{Eu}^{2+},\text{Mn}^{2+}$  phosphors for near-UV white LEDs," *Dalton Transactions*, vol. 44, no. 33, pp. 15006–15013, 2015.
- [2] A. Canimoglu, J. Garcia-Guinea, Y. Karabulut, M. Ayvacikli, A. Jorge, and N. Can, "Catholuminescence properties of rare earth doped  $\text{CaSnO}_3$  phosphor," *Applied Radiation and Isotopes*, vol. 99, pp. 138–145, 2015.
- [3] D. Zhang, M. Shi, Y. Sun, Y. Guo, and C. Chang, "Long afterglow property of  $\text{Er}^{3+}$  doped  $\text{Ca}_2\text{SnO}_4$  phosphor," *Journal of Alloys and Compounds*, vol. 667, pp. 235–239, 2016.
- [4] F. Zhong, H. Zhuang, Q. Gu, and J. Long, "Structural evolution of alkaline earth metal stannates  $\text{MSnO}_3$  ( $\text{M}=\text{Ca}$ ,  $\text{Sr}$ , and  $\text{Ba}$ ) photocatalysts for hydrogen production," *RSC Advances*, vol. 6, no. 48, pp. 42474–42481, 2016.
- [5] J. Xie, Y. Shi, F. Zhang, and G. Li, " $\text{CaSnO}_3:\text{Tb}^{3+}, \text{Eu}^{3+}$ : a distorted-perovskite structure phosphor with tunable photoluminescence properties," *Journal of Materials Science*, vol. 51, no. 16, pp. 7471–7479, 2016.
- [6] K. V. Dabre and S. J. Dhoble, "Synthesis and photoluminescence properties of  $\text{Eu}^{3+}$ ,  $\text{Sm}^{3+}$  and  $\text{Pr}^{3+}$  doped  $\text{Ca}_2\text{ZnWO}_6$  phosphors for phosphor converted LED," *Journal of Luminescence*, vol. 150, pp. 55–58, 2014.
- [7] L. Jiang, R. Pang, D. Li et al., "Tri-chromatic white-light emission from a single-phase  $\text{Ca}_9\text{Sc}(\text{PO}_4)_7:\text{Eu}^{2+},\text{Tb}^{3+},\text{Mn}^{2+}$  phosphor for LED applications," *Dalton Transactions*, vol. 44, no. 39, pp. 17241–17250, 2015.
- [8] L. K. Bharat, S. K. Jeon, K. G. Krishna et al., "Rare-earth free self-luminescent  $\text{Ca}_2\text{KZn}_2(\text{VO}_4)_3$  phosphors for intense white light-emitting diodes," *Science Reports*, vol. 7, no. 1, 2017.
- [9] M. S. Mendhe, S. P. Puppallwar, and S. J. Dhoble, "Novel single-component  $\text{CaLaAlO}_4:\text{Tb}^{3+}, \text{Eu}^{3+}$  phosphor for white light-emission," *Optical Materials*, vol. 82, pp. 47–55, 2018.
- [10] X. Bian and J. Zhang, "White-light emission in a single-phase  $\text{Ca}_9.3\text{Mg}_0.7\text{K}(\text{PO}_4)_7:\text{Eu}^{2+},\text{Tb}^{3+}, \text{Mn}^{2+}$ , phosphor for light-emitting diodes," *Journal of Luminescence*, vol. 194, pp. 334–340, 2017.
- [11] X. Huang and H. Guo, "Synthesis and photoluminescence properties of  $\text{Eu}^{3+}$ -activated  $\text{LiCa}_3\text{ZnV}_3\text{O}_{12}$  white-emitting phosphors," *RSC Advances*, vol. 8, no. 31, 2018.
- [12] T. Hasegawa, Y. Abe, A. Koizumi et al., "Bluish-white luminescence in rare-earth-free vanadate garnet phosphors: structural characterization of  $\text{LiCa}_3\text{MV}_3\text{O}_{12}$  ( $\text{M}=\text{Zn}$  and  $\text{Mg}$ )," *Inorganic Chemistry*, vol. 57, no. 2, pp. 857–866, 2018.
- [13] P. Dang, S. Liang, G. Li et al., "Full color luminescence tuning in  $\text{Bi}^{3+}/\text{Eu}^{3+}$ -doped  $\text{LiCa}_3\text{MgV}_3\text{O}_{12}$  garnet phosphors based on local lattice distortion and multiple energy transfers," *Inorganic Chemistry*, vol. 57, no. 15, pp. 9251–9259, 2018.
- [14] J. J. Wei, K. Korthout, D. Poelman, and P. F. Smet, "Origin of saturated green emission from europium in zinc thiogallate," *Optical Materials Express*, vol. 3, no. 9, p. 1338, 2013.
- [15] P. S. Tung, L. T. T. Hien, N. N. Ha, T. N. Khiem, and N. D. Chien, "Influence of composition, doping concentration and annealing temperatures on optical properties of  $\text{Eu}^{3+}$ -



- doped ZnO-SiO<sub>2</sub> nanocomposites,” *Journal of Nanoscience and Nanotechnology*, vol. 16, no. 8, pp. 7955–7958, 2016.
- [16] F. Lei, L.-J. Huang, Y. Shi, J.-J. Xie, L. Zhang, and W. Xiao, “Molten salt synthesis of color-tunable and single-component NaY(1-x-y)(WO<sub>4</sub>)<sub>2</sub>:Eu<sup>3+</sup>, x, Tb<sup>3+</sup>, y, phosphor for UV LEDs,” *Journal of Materials Research*, vol. 32, no. 8, pp. 1548–1554, 2017.
- [17] S. Xu, Z. Wang, P. Li et al., “Single-phase white-emitting phosphors Ba<sub>3</sub>Ce(1-x-y)(PO<sub>4</sub>)<sub>3</sub>:xTb<sup>3+</sup>,yMn<sup>2+</sup> and Ba<sub>3</sub>Ce(1-x-z)(PO<sub>4</sub>)<sub>3</sub>:xTb<sup>3+</sup>,zSm<sup>3+</sup>: structure, luminescence, energy transfer and thermal stability,” *RSC Advances*, vol. 7, no. 32, pp. 19584–19592, 2017.
- [18] B. Tian, B. Chen, Y. Tian et al., “Excitation pathway and temperature dependent luminescence in color tunable Ba<sub>5</sub>Gd<sub>8</sub>Zn<sub>4</sub>O<sub>21</sub>:Eu<sup>3+</sup> phosphors,” *Journal of Materials Chemistry C*, vol. 1, no. 12, p. 2338, 2013.
- [19] Y. Tian, B. Chen, R. Hua et al., “Optical transition, electron-phonon coupling and fluorescent quenching of La<sub>2</sub>(MoO<sub>4</sub>)<sub>3</sub>:Eu<sup>3+</sup> phosphor,” *Journal of Applied Physics*, vol. 109, no. 5, p. 053511, 2011.
- [20] L. Han, G. Liu, X. Dong, J. Wang, and W. Yu, “Single-phase and warm white-light-emitting phosphors CaLa<sub>2</sub>-(MoO<sub>4</sub>)<sub>4</sub>: xDy<sup>3+</sup>, yEu<sup>3+</sup>: synthesis, luminescence and energy transfer,” *Journal of Luminescence*, vol. 178, pp. 61–67, 2016.
- [21] Z. Hu, Y. Guo, J. Zhang, and Y. Zhang, “Tunable luminescence properties and energy transfer of single-phase Ca<sub>4</sub>(PO<sub>4</sub>)<sub>2</sub>O: Dy<sup>3+</sup>, Eu<sup>2+</sup> multi-color phosphors for warm white light,” *Journal of Materials Science*, vol. 53, no. 9, pp. 6414–6423, 2018.
- [22] K. K. Nishad, J. Joseph, N. Tiwari, R. Kurchania, and R.K. Pandey, “Investigation on size dependent elemental binding energies and structural properties of ZnO nanoparticles and their correlation with observed photo-luminescence behavior,” *Science of Advanced Materials*, vol. 7, no. 7, 2015.